ENVIRONMENTAL RESEARCH
WATER

PURPOSE-LED PUBLISHING™

Part of the ENVIRONMENTAL RESEARCH SERIES

PAPER • OPEN ACCESS

Future nutrient reduction needs in world's largest rivers to limit coastal eutrophication

To cite this article: Albert Nkwasa *et al* 2026 *Environ. Res.: Water* **2** 025004

View the article online for updates and enhancements.

IOP Publishing Environ. Res.: Water 2 (2026) 025004 https://doi.org/10.1088/3033-4942/ae54c3

ENVIRONMENTAL RESEARCH
WATER

Check for updates

OPEN ACCESS

RECEIVED
30 June 2025

REVISED
10 February 2026

ACCEPTED FOR PUBLICATION
19 March 2026

PUBLISHED
10 April 2026

PAPER

Future nutrient reduction needs in world's largest rivers to limit coastal eutrophication

Albert Nkwasa[1,2,*], **Maria Theresa Nakkazi**[2], **Celray James Chawanda**[2,3], **Ting Tang**[4], **Keerthana Suresh**[1,5], **Arthur H W Beusen**[6,7], **Ilaria Micella**[8], **Maryna Strokal**[8], **Taher Kahil**[1,9] and **Ann van Griensven**[2,10]

[1] Water Security Research Group, Biodiversity and Natural Resources Program, International Institute for Applied Systems Analysis (IIASA), Schlossplatz 1, A-2361 Laxenburg, Austria
[2] Department of Water and Climate, Vrije Universiteit Brussel (VUB), 1050 Brussel, Belgium
[3] Texas A&M AgriLife Research, Blackland Research & Extension Center, Temple, TX 76502, United States of America
[4] Biological and Environmental Science and Engineering Division, King Abdullah University of Science and Technology, Thuwal, Saudi Arabia
[5] Department of Physical Geography, Faculty of Geosciences, Utrecht University, Utrecht, The Netherlands
[6] Department of Earth Sciences, Faculty of Geosciences, Utrecht University, Utrecht, The Netherlands
[7] PBL Netherlands Environmental Assessment Agency, The Hague, The Netherlands
[8] Earth Systems and Global Change Group, Wageningen University & Research, Wageningen, The Netherlands
[9] United Nations University Institute for Water, Environment and Health (UNU-INWEH), Hamilton, ON, Canada
[10] Water Science & Engineering Department, IHE Delft Institute for Water Education, 2611 AX Delft, The Netherlands
[*] Author to whom any correspondence should be addressed.

E-mail: nkwasa@iiasa.ac.at

Keywords: coastal eutrophication, riverine nutrient export, nutrient load reduction, global water quality modeling

Supplementary material for this article is available online

Abstract

Riverine exports of total nitrogen (TN) and total phosphorus (TP) are major drivers of coastal eutrophication. However, few studies have quantified the reductions required to mitigate future eutrophication risks under changing socio-economic and climatic conditions. Here, we use three global water quality models (Integrated Model to Assess the Global Environment-Dynamic Global Nutrient Model, CoSWAT-WQ, and MARINA-Multi) to project TN and TP export loads from twenty four of the world's largest river basins under a high-emission and high socio-economic growth scenario (SSP5-Representative Concentration Pathways 8.5). Our multi-model mean projections indicate that TN and TP exports from these basins could increase by 18% and 21%, respectively, by 2050 relative to 2010 export levels. To avoid the risk of future coastal eutrophication, we estimate reductions in TN and TP riverine exports to coastal waters of approximately 67% and 64%, respectively by 2050. In particular, major river basins such as the Nile, Niger, Yangtze, Ganges, Danube, São Francisco, and Zhujiang will require nutrient load reductions exceeding 50% for both TN and TP. Ultimately, achieving the necessary nutrient reductions will require coordinated, targeted interventions to protect our global coastal ecosystems. Meanwhile, the variability among model simulations underscores the need to advance global water quality modeling frameworks to reduce uncertainties and better support science-based policy making.

1. Introduction

Rivers serve as the primary conduits for transporting anthropogenic materials from terrestrial environments to coastal waters, significantly influencing marine biogeochemical cycles (Sharples *et al* 2017). Anthropogenic activities, particularly wastewater discharge and agricultural intensification, have substantially increased riverine nutrient loads, primarily nitrogen (N) and phosphorus (P) (McDowell *et al* 2025). Additionally, anthropogenic sources are projected to become increasingly dominant by 2050, accounting for up to 80% of riverine nutrients delivery to coastal waters globally, while natural nutrient sources continue to decline across all Shared Socioeconomic Pathways due to land-use transformations

(Beusen *et al* 2022). These elevated riverine nutrient inputs, when transported to coastal waters, transform previously pristine coastal waters into mesotrophic and eutrophic conditions, leading to shifts in food web structures, biodiversity loss, proliferation of harmful algal blooms, and decline in fish stocks (Rousseau *et al* 2000, Kemp *et al* 2009, Diaz *et al* 2011, Tong *et al* 2015, Maúre *et al* 2021).

Nutrient transport models that quantify nutrient fluxes to surface waters and their effects on coastal waters can provide important inputs for assessing the risk of coastal eutrophication (Billen and Garnier 2023, Ural-Janssen *et al* 2024). Several nutrient models have been developed and applied across spatial scales, ranging from global to regional and local applications (e.g. Grizzetti *et al* 2008, Yasin *et al* 2010, Malagó *et al* 2017, Fink *et al* 2018). Additionally, these nutrient models have been widely employed to project future nutrient loadings under multiple global change scenarios (Bak *et al* 2025, Elsayed *et al* 2025). However, while significant efforts have been made to project future riverine N and P loads, little attention has been given to backcasting nutrient exports to determine the required reductions in river nutrient loading to mitigate the risk of coastal eutrophication.

Backcasting is a methodological approach that involves working backwards from a particular desired end-point to the present, in order to determine what measures would be required to reach that point (Robinson 1990, Gomi *et al* 2011). In our context, backcasting entails estimating future nutrient loadings and determining the extent of nutrient reductions required to avoid the risk of coastal eutrophication. A commonly used proxy for assessing coastal eutrophication risk is the Indicator for Coastal Eutrophication Potential (ICEP) (Billen and Garnier 2007), which is derived from the Redfield ratio (Redfield *et al* 1963). It serves as a key metric for reporting on SDG 14.1.1(a), providing insights into the state of oceans within the framework of the Sustainable Development Goals (UNEP 2021). The ICEP expresses nutrient imbalance of N and P in river water flowing into the coastal waters relative to silicon (Si) availability, as excess N and/or P can promote the growth of non-siliceous algae at the expense of diatoms, increasing the likelihood of harmful algal blooms (Billen and Garnier 1997, Garnier *et al* 2010). Only a few studies have applied backcasting approaches to reconstruct historical nutrient loads in river systems, and have primarily relied on ICEP (Li *et al* 2019, Ural-Janssen *et al* 2024). As a result, estimates of the required reductions of both total nitrogen (TN) and total phosphorus (TP), calculated with backcasting, based on multi-model projections for major large river basins worldwide have been limited.

In this study, we address this gap by estimating the reductions required to avoid the risk of coastal eutrophication in the world's largest twenty four rivers by 2050 under a high-emission and high-socio-economic growth scenario Representative Concentration Pathways (SSP5-RCP8.5), characterized by rapid, fossil-fueled economic growth. These rivers were selected based on a basin area greater than 400 000 km^2 and an average annual discharge exceeding 3900 $m^3\ s^{-1}$. Large rivers are of particular interest because they deliver the highest absolute nutrient loads to coastal waters and most are already impacted by nutrient enrichment (Best 2019). To project N and P exports for 2050 relative to a 2010 baseline, we use simulations from three global nutrient models i.e. Integrated Model to Assess the Global Environment-Dynamic Global Nutrient Model (IMAGE-DGNM) (Beusen *et al* 2022), CoSWAT-WQ (Nkwasa *et al* 2025) and MARINA-Multi (Micella *et al* 2024a). We then apply a backcasting approach to identify the nutrient reductions needed to limit the risk of coastal eutrophication by mid-century. Estimating these nutrient reductions is crucial for quantifying the progress required and to implement effective mitigation strategies to prevent future coastal eutrophication.

2. Materials and methods

2.1. Selected large rivers

We focused on 24 major river basins (table 1), including the Amazon, Nile, Congo, Mississippi, Ob, Parana, Yenisey, Lena, Niger, Yangtze, Amur, Mackenzie, Ganges, Zambezi, Nelson, St. Lawrence, Orinoco, Danube, Tocantins, Mekong, Columbia, São Francisco, Zhujiang, and Irrawaddy. This set provides global coverage of the world's largest river systems, which are consistently represented in global-scale nutrient models and together account for most of the riverine nutrient fluxes to coastal waters (Mayorga *et al* 2010, Best 2019). Restricting the analysis to large river basins also minimizes uncertainties associated with smaller catchments, where model outputs are highly sensitive to fine-scale variability in hydrology, land use, and water infrastructure.

2.2. Models and data

Three global water quality models (table 2) used in this study are the IMAGE-DGNM (Beusen *et al* 2022), CoSWAT-WQ (Nkwasa *et al* 2025) and MARINA-Multi (Micella *et al* 2024a). IMAGE-DGNM is

Table 1. Key characteristics of the 24 selected large river basins, including basin area (Seitzinger *et al* 2010, Best 2019), population (Best 2019), mean annual flow (Milliman and Farnsworth 2011, Best 2019), multi-model mean TN and TP loadings for 2010 (Beusen *et al* 2022, Micella *et al* 2024b, Nkwasa *et al* 2025), and main anthropogenic nutrient sources (Micella *et al* 2024a).

River ID	River name	Continent	Basin area (10^6 km^2)	Population (10^6)	Mean annual flow (10^3 m^3 s^{-1})	TN (Tg yr^{-1})	TP (Tg yr^{-1})	Major anthropogenic source
1	Amazon	South America	5.85	32.16	199.77	3.38	0.38	Diffuse
2	Nile	Africa	3.82	174.37	2.54	0.69	0.05	Diffuse and point sources
3	Congo	Africa	3.69	90.61	41.22	0.98	0.10	Diffuse
4	Mississippi	North America	3.20	68.17	15.54	1.20	0.09	Diffuse
5	Ob	Asia	3.02	30.70	12.37	0.23	0.16	Point sources
6	Parana	South America	2.66	88.22	16.81	0.63	0.09	Diffuse
7	Yenisey	Asia	2.58	7.80	19.66	0.0003	0.02	Point sources
8	Lena	Asia	2.44	0.24	16.49	0.0002	0.03	Point sources
9	Niger	Africa	2.24	93.62	6.03	0.29	0.05	Diffuse
10	Yangtze	Asia	1.79	586.01	28.54	2.74	0.49	Diffuse
11	Amur	Asia	1.75	65.21	11.10	1.48	0.09	Diffuse
12	Mackenzie	North America	1.69	0.30	9.83	0.06	0.02	Point sources
13	Ganges	South Asia	1.63	477.94	15.54	1.86	0.48	Diffuse
14	Zambezi	Africa	1.36	37.98	3.17	0.12	0.01	Diffuse
15	Nelson	North America	1.14	0.32	2.37	0.10	0.00	Diffuse
16	St. Lawrence	North America	1.05	45.87	10.78	0.07	0.04	Point sources
17	Orinoco	South America	1.04	12.16	34.88	0.69	0.10	Diffuse
18	Danube	Europe	0.79	80.19	6.66	0.49	0.06	Diffuse
19	Tocantins	South America	0.77	1.51	11.00	0.43	0.05	Diffuse
20	Mekong	Asia	0.76	58.74	17.44	0.55	0.07	Diffuse
21	Columbia	North America	0.73	7.49	7.61	0.45	0.07	Point sources
22	Sao Francisco	South America	0.61	14.61	2.70	0.10	0.02	Diffuse
23	Zhujiang	Asia	0.41	74.90	8.25	0.73	0.14	Diffuse
24	Irrawaddy	Asia	0.41	28.58	13.64	0.40	0.05	Diffuse

Table 2. Global water quality models used in this study under SSP5-RCP8.5 scenario.

Model	Constituent used	Discretization	Temporal resolution	Common time period	Key reference
IMAGE-DGNM	TN, TP	Grid (0.5 degrees)	Yearly	2010, 2050	Beusen *et al* (2022)
CoSWAT-WQ	TN, TP	HRU (0.5 degrees)	Daily	2010, 2050	Nkwasa *et al* (2025)
MARINA-Multi	TDN, TDP	Sub-basin	Multi-year	2010, 2050	Micella *et al* (2024a, 2024b)

a spatially explicit, dynamic model that simulates nutrient delivery from diffuse (agriculture, natural ecosystems, aquaculture, weathering, deposition) and point (sewage) sources. It tracks nutrient transport through groundwater, surface water, and atmospheric pathways, considering long-term accumulation and storage. The model estimates nutrient budgets, leaching, retention, and riverine transport, integrating land use and hydrological dynamics. IMAGE-GNM uses the grid-based global hydrological model PCRaster Global Water Balance (Sutanudjaja *et al* 2018) to quantify water and nutrient fluxes through streams and rivers, lakes, wetlands and reservoirs. The IMAGE-DGNM model has been evaluated against long-term observations from major rivers (Meuse, Rhine, Mississippi, Yangtze) and across tropical and temperate systems, showing RMSE (root mean square error) values of 18%–46% for N and 38%–323% for P, and successfully reproducing multi-decadal trends without bias, supporting large-scale scenario assessments (Beusen *et al* 2022). The simulation results used in this study for IMAGE-DGNM are taken from Beusen *et al* (2022). A detailed description and validation of this model can be found in Beusen *et al* (2015) and Beusen *et al* (2022).

CoSWAT-WQ model is a community global Soil and Water Assessment Tool (SWAT+) (Nkwasa *et al* 2025). SWAT+ is an enhanced version of the SWAT model (Arnold *et al* 1998), designed to offer greater flexibility in connecting spatial units and modeling nutrient management practices (Bieger *et al* 2017). It is a semi-distributed model that simulates hydrological dynamics, crop growth, sediment transport, and nutrient loads by dividing hydrological basins into sub-basins and Hydrologic Response Units (HRUs). The model also distinguishes upland and lowland processes through landscape units and relies on the water balance concept as the foundation for all hydrological processes (Nkwasa *et al* 2022). It simulates N and P cycles, tracking both inorganic and organic forms of these nutrients at the land phase, with in-stream nutrient dynamics modeled at the river phase using the kinetic routines from the QUAL2E in-stream water quality model (Brown and Barnwell 1987). Dissolved nutrients are carried by water flow, while sediment-bound nutrients are either transported with the water or settle on the channel bed. The CoSWAT-WQ model has been evaluated against *in-situ* observations from the Global Environment Monitoring System for Freshwater's (GEMS/Water) database (GEMStat), achieving nRMSE (normalized RMSE) < 1 at over 80% of gauging stations for TN and TP, and its performance is consistent with other global and regional nutrient models (Nkwasa *et al* 2024), supporting its applicability for large-scale nutrient assessments. Further details on the scenario setup and evaluation of the CoSWAT-WQ model are provided in Nkwasa *et al* (2025).

The MARINA-Multi model (Model to Assess River Inputs of pollutants to the seas) (Micella *et al* 2024a) quantifies river exports of nutrients (N and P) to coastal waters at the sub-basin level. The model simulates this from 10 226 sub-basins, incorporating point sources (treated and untreated sewage, direct manure discharge) and diffuse sources (natural and anthropogenic). Nutrient exports by rivers are modeled as dissolved inorganic nitrogen, dissolved inorganic phosphorus, dissolved organic nitrogen, and dissolved organic phosphorus. Total dissolved nitrogen (TDN) and total dissolved phosphorus (TDP) are then computed based on these individual components (Strokal *et al* 2016). Natural river discharge is used from the Variable Infiltration Capacity hydrological model (van Vliet *et al* 2013). The MARINA-Multi model has been evaluated against observational datasets (e.g. ∼2000 GEMStat observations) and shows good agreement for riverine nitrogen (R^2 = coefficient of determination, 0.73–0.76; NSE = Nash–Sutcliffe efficiency, 0.61–0.63) and phosphorus ($R^2 = 0.57$–0.61; NSE = 0.45–0.53), and further comparison with other global and regional nutrient models demonstrate its robustness for large-scale nutrient assessments (Micella *et al* 2024b). For more details on the scenario setup and evaluation of the MARINA-Multi model, refer to Micella *et al* (2024a) and Micella *et al* (2024b). Since the MARINA-Multi model simulates TDN and TDP, we converted these values to TN and TP using the following conversion factors; TN = TDN*1.1 and TP = TDP*1.7 (de Klein and Koelmans 2011). While these ratios are specifically validated for European rivers, we apply them to all rivers in our study. This approach provides a consistent method for comparing TN and TP load simulations across the three models, although it may introduce some uncertainties, which could be considered a potential limitation.

Using the same scenario assumptions as model inputs is essential to ensure inter-model consistency and enable comparison of model outcomes across scales and constituents. Here, the models of this study consistently used a set of socio-economic scenario assumptions and data sets based on the SSPs, SSP5 and climate data from the RCP 8.5, for computing future water quality. SSP5 is characterized by high socio-economic growth with heavy fossil fuel use and increased high-tech agricultural production (O'Neill *et al* 2017), whereas RCP8.5 considers a high level of greenhouse gas emissions (Van Vuuren *et al* 2011). Even though the same scenario was selected, all the three models used different implementations for estimating future diffuse and point source inputs described in the key references (table 2) and summarized in table S1 of the Supplementary material. While not formally calibrated globally, these models have been extensively validated and widely applied to simulate long-term nitrogen and phosphorus trends (Strokal *et al* 2025). Their ability to reproduce observed large-scale patterns supports their use for scenario analysis, and combining them in an ensemble further strengthens the results by capturing structural differences and increasing confidence in the projections.

2.3. Ensemble statistics (multi-model mean)

To reduce the influence of interannual variability, the reported nutrient loads for 2010 and 2050 represent 10 year averages centered on the target year. For CoSWAT-WQ and IMAGE-DGNM, simulated loads from five years before to five years after the target year (i.e. 2005–2015 for 2010 and 2045–2055 for 2050) were averaged. For MARINA-Multi, we used the simulated loads for the target year, which were forced with averaged discharge data over the corresponding 10 year periods.

Using these averaged representative year nutrient loads, statistics across the multi-model ensemble were computed after calculating the respective metrics. For example, the relative change (%) in TN and TP load exports between 2010 and 2050 was first calculated individually for each model combination. Subsequently, the multi-model mean and agreement were determined across the three water quality models for the selected rivers. An example for the Mekong River illustrating the multi-model mean calculation is presented in figure S1, supplementary material. We also evaluated the confidence of model-derived estimates using an agreement metric that incorporates both the direction and the magnitude of projected changes. For each river basin, we assessed whether two or all three models agreed on (i) the sign of change and (ii) the range of magnitude of change. This approach follows the principle that robust ensemble interpretation requires consistency in both direction and magnitude (Knutti *et al* 2010, Maher *et al* 2021). Confidence levels were classified into three categories: (1) high confidence, defined as basins where all three models agree on the sign of change and at least two models agree on the magnitude range; (2) moderate confidence, defined as basins where two models agree on both the sign of change and the magnitude range or where all three models agree on the sign of change but no pair agrees on magnitude ranges; and (3) low confidence, defined as basins where two models agree on the sign of change but do not agree on the magnitude range.

2.4. Coastal eutrophication potential and backcasting approach

We used the ICEP (Billen and Garnier 2007) to represent the risks of coastal eutrophication by 2050 for the selected major rivers globally. The ICEP value is calculated based on the molar Redfield ratio, C:N:P:Si = 106:16:1:20 indicating the potential development of the non-siliceous algae (e.g. cyanobacteria) in coastal water that can be harmful. A low risk of coastal eutrophication is indicated when the ICEP value is below zero; in other words, an ICEP value of greater than zero results in excess nutrients (N, P) over silicon. To apply our backcasting approach, first, we quantified the maximum allowable river exports of TN and TP (equations (1) and (2) respectively) to oceans by targeting the ICEP as '0' to ensure low risks of coastal eutrophication following the approaches of Li *et al* (2019) and Ural-Janssen *et al* (2024), using an uncertainty range of '−2' and '+2',

$$\mathrm{TN_{max}} = \left(\frac{\mathrm{ICEP_N}}{106 \times 12} + \frac{\mathrm{Si_{fx}}}{28 \times 20}\right) \times (14 \times 16) \tag{1}$$

$$\mathrm{TP_{max}} = \left(\frac{\mathrm{ICEP_P}}{106 \times 12} + \frac{\mathrm{Si_{fx}}}{28 \times 20}\right) \times (31) \tag{2}$$

where; $\mathrm{ICEP_N} = 0$ (−2 and +2), $\mathrm{ICEP_P} = 0$ (−2 and +2) kg C $\mathrm{km^{-2}\ d^{-1}}$, $\mathrm{TN_{max}}$ and $\mathrm{TP_{max}}$ are the maximum allowable river export of TN and TP (kg N or P $\mathrm{km^{-2}\ d^{-1}}$) by 2050, and $\mathrm{Si_{fx}}$ is the total dissolved Silica (DSi) flux to oceans by rivers (kg Si $\mathrm{km^{-2}\ d^{-1}}$) for 2050. The DSi data for the selected rivers was obtained from the Global NEWS-2 model for 2050, using the Global Orchestration (GO) scenario (Seitzinger *et al* 2010). This scenario depicts a globally connected society focused on trade and economic liberalization, taking a reactive approach to ecosystem issues. It is the closest match to the SSP5-RCP8.5 scenario. To our knowledge, no other globally projected DSi data is available. Next, we performed backcasting calculations by determining the difference between the projected nutrient load for 2050 and the maximum allowable nutrient load for 2050. This difference gives a projection of how much nutrient load reductions will be required to avoid the risk of future coastal eutrophication. This backcasting effectively informs how much each river's nutrient load must be reduced from the projected nutrient load under SSP5-RCP8.5 for a low eutrophication risk.

3. Results

3.1. Multi-model TN and TP export changes

Overall, between 2010 and 2050, the multi-model mean relative change in TN and TP load exports across the 24 selected rivers is estimated at 18% and 21%, respectively. All models project an increase in both TN and TP exports by 2050 compared to the baseline year of 2010 (figure 1). In 2010, model simulations of TN export range between 13.0–18.3 Tg N $\mathrm{yr^{-1}}$, while TP export ranges between 1.1–2.6 Tg P $\mathrm{yr^{-1}}$. By 2050, TN load export is projected to be 16.3–20.5 Tg N $\mathrm{yr^{-1}}$, and TP export is projected to be 1.5–3.2 Tg P $\mathrm{yr^{-1}}$ across the three models (figure 1). The consistent direction of change and the close agreement in magnitude across the three models indicates a relatively high level of confidence in the projected increases. The projected increases in TN and TP exports by 2050 are primarily attributed to continued agricultural nutrient inputs especially in regions such as Europe, India, China, and Sub-Saharan Africa, and are further intensified by rising sewage-related discharges under the SSP5 scenario, driven by the rapid expansion of urban populations (Beusen *et al* 2022, Micella *et al* 2024b, Nkwasa *et al* 2025).

Examining the spatial distribution of relative changes in TN and TP load exports for 2050 compared to the baseline year of 2010 (figure 2), the multi-model mean across all global water quality models reveals several consistent large-scale patterns. Specifically, nutrient loading (Tg $\mathrm{yr^{-1}}$) is projected to increase by more than 10% in 13 rivers (i.e. more than half of the selected rivers) for TN and in 12 rivers (i.e. half of the selected rivers) for TP by 2050, relative to 2010 (figure 2). About one third of the selected basins exhibit changes within ±10%. Rivers projected to experience the greatest increases (>50%) in both TN and TP load exports include the Nile, Congo, Niger, Ganges,

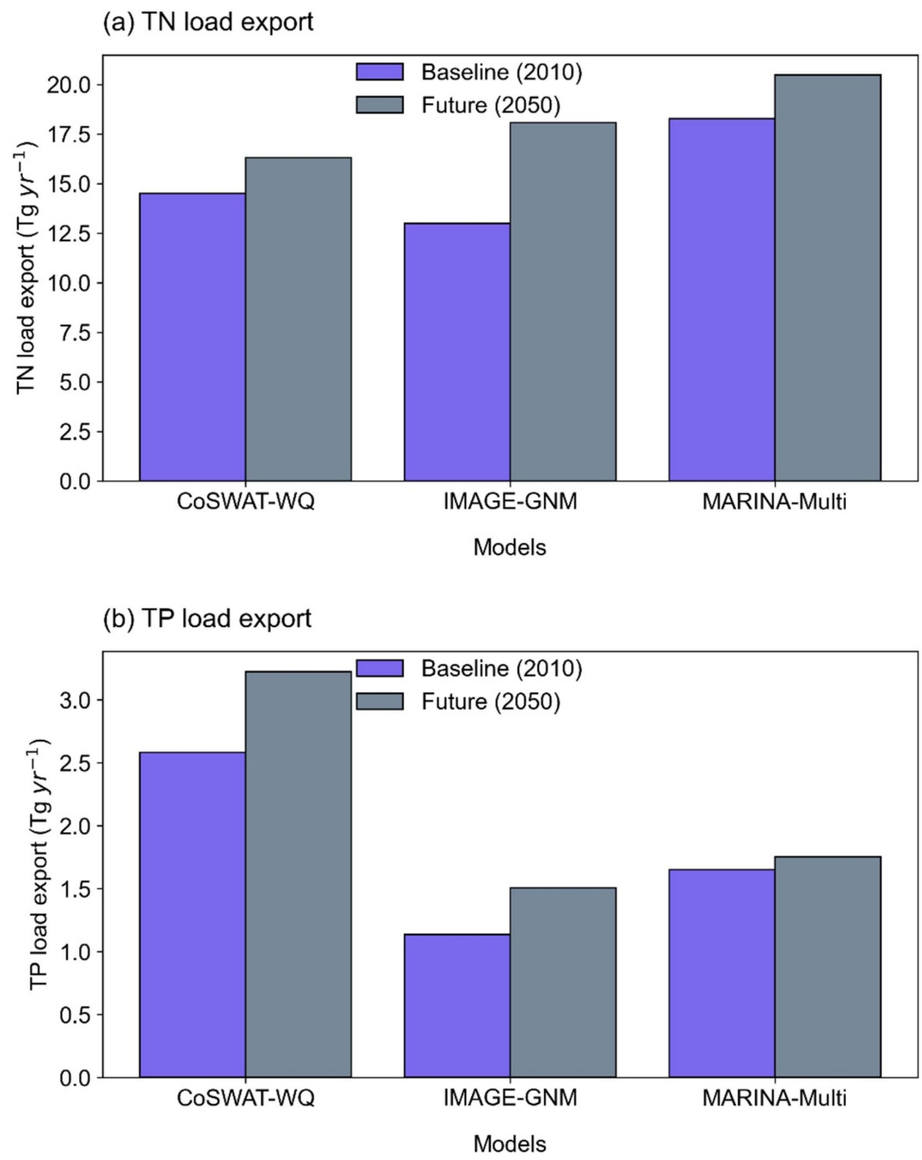

Figure 1. Total average annual inter-model river load export for (a) TN and (b) TP in 2010 and 2050 under SSP5-RCP8.5 for the 24 largest river basins.

Zambezi, and Irrawaddy, with the Mekong additionally showing a >50% increase in TP export only (figures 2(a) and (b)).

Regarding confidence levels in model agreement on both the direction and magnitude of projected changes, high confidence is observed for the Zambezi, Niger, St. Lawrence, Orinoco, São Francisco, Paraná, Yenisey, Ganges, Mekong, and Irrawaddy basins. In contrast, the Ob and Amur basins exhibit low confidence while the remaining basins show moderate confidence levels (figure 3(a)). For TP, high confidence among the three models is found for the Nile, Congo, Niger, Mississippi, St. Lawrence, Orinoco, São Francisco, Paraná, Ob, Yenisey, Lena, Ganges, Mekong, and Irrawaddy basins. The Zhujiang basin, however, shows low confidence, and other basins fall within a moderate range (figure 3(b)).

3.2. Required reductions to avoid coastal eutrophication

To achieve the maximum allowable nutrient export levels by 2050, substantial reductions of over 50% are needed in most rivers to mitigate eutrophication risks (figures 4 and 5). For TN, major reductions are needed in rivers including the Nile, Niger, Yangtze, Amur, Ganges, Nelson, Orinoco, Danube, Tocantins, São Francisco, and Zhujiang (figure 4). Similarly, for TP, significant reductions are required in the Nile, Congo, Ob, Niger, Yangtze, Ganges, St. Lawrence, Danube, Tocantins, São Francisco, and Zhujiang (figure 5). Globally, considering all the rivers shown in figures 4 and 5 that require nutrient reductions to meet the maximum allowable export levels by 2050, substantial total reductions of

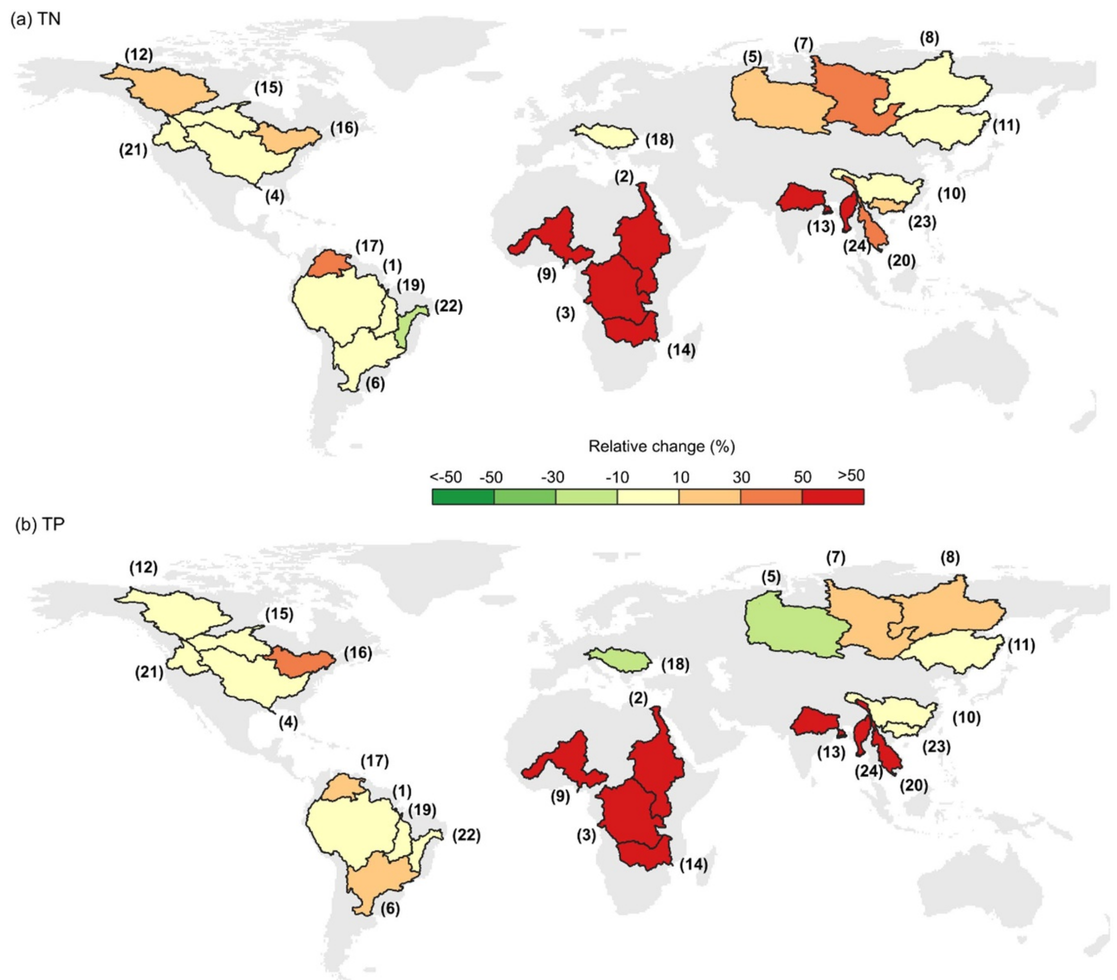

Figure 2. Average relative change in (a) TN and (b) TP river loading to coastal zones between 2010 and 2050 under SSP5-RCP8.5, based on three models. Outlets of rivers are numbered: 1—Amazon, 2—Nile, 3—Congo, 4—Mississippi, 5—Ob, 6—Parana, 7—Yenisey, 8—Lena, 9—Niger, 10—Yangtze, 11—Amur, 12—Mackenzie, 13—Ganges, 14—Zambezi, 15—Nelson, 16—St. Lawrence, 17—Orinoco, 18—Danube, 19—Tocantins, 20—Mekong, 21—Columbia, 22—Sao Francisco, 23—Zhujiang, 24—Irrawaddy.

over 67% and 64% in riverine exports of TN and TP, respectively, are needed to prevent future coastal eutrophication under the SSP5-RCP8.5 scenario (figures S2 and S3).

Interestingly, some rivers like the Irrawaddy are projected to experience a significant increase in TN export (>50%) by 2050 but do not require major reductions. A similar pattern is observed for TP where the Irrawaddy and Mekong show large projected increases (>50%) by 2050 but do not appear to need major TP reductions. This may suggest that these rivers continue to export enough DSi to maintain nutrient ratios below eutrophication thresholds, as defined by the ICEP for N and P.

In contrast, some rivers such as the Danube, Nelson, Columbia, Tocantins, São Francisco, and Zhujiang are projected to have relatively small changes in nutrient export (±10% by 2050), yet still require reductions greater than 50% to limit coastal eutrophication. This highlights that even modest changes in nutrient loads can still pose a significant threat to coastal ecosystems if baseline exports are already high or if nutrient ratios are unbalanced. Overall, these results illustrate the diversity in required nutrient reductions across major river basins. They also emphasize the need to assess both nitrogen and phosphorus when evaluating eutrophication risks, as the reductions required for each nutrient often differ.

4. Discussion

4.1. Results in global perspective

The simulated total nutrient exports from the twenty four large river basins included in this analysis account for approximately half of the global riverine TN and TP exports reported in previous studies.

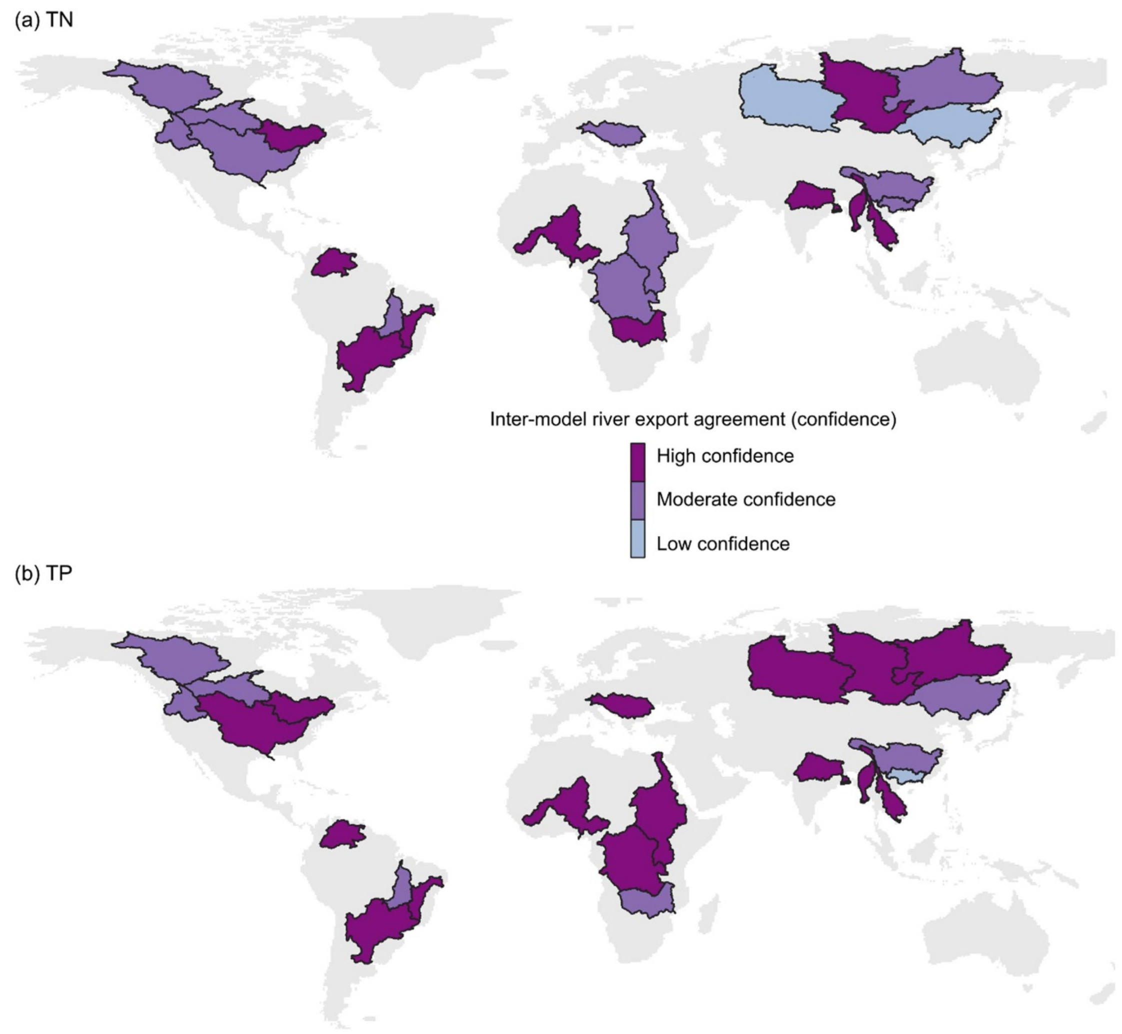

Figure 3. Inter-model confidence in (a) TN and (b) TP estimates across river basins, based on the agreement among the three models in sign direction and magnitude of change. Higher confidence indicates stronger model consistency in sign and magnitude of change.

For the baseline year 2010, we simulate a multi-model mean export of 16 Tg N yr^{-1} and 1.8 Tg P yr^{-1} (figure 1). These values correspond to approximately 44% and 46% of the global TN and TP exports to coastal waters reported by Beusen *et al* (2022), who simulated 36.5 Tg N yr^{-1} and 3.9 Tg P yr^{-1} globally, respectively. In the absence of harmonized global simulations for the year 2010 from other models, we also refer to simulations from earlier studies centered around the year 2000, including 40 Tg N yr^{-1} (Green *et al* 2004), 43 Tg N yr^{-1} from Global NEWS, and up to 60 Tg N yr^{-1} from an earlier version of Global NEWS (Seitzinger *et al* 2005). For TP, our simulation is considerably lower than the 9 Tg P yr^{-1} reported for the year 2000 by Seitzinger *et al* (2005). While these reference values do not correspond exactly to our baseline year, they represent the most widely cited global estimates available and are therefore used to provide contextual interpretation, acknowledging the inherent temporal mismatch. These differences in reported TN and TP exports underscore the substantial uncertainty associated with global nutrient modeling, driven by variability in model structures, input data quality, and assumptions regarding nutrient sources, transport, and retention processes (supplementary material, table S1).

4.2. Multi-model estimates

All models consistently project the same overall direction of change in future TN and TP loads; however, at the level of individual river basins, discrepancies in the direction and magnitude of change are observed, resulting in varying levels of confidence in projected estimates. For TN, high inter-model confidence is achieved in 10 river basins (42%), while moderate inter-model confidence is achieved in 13 basins (54%). For TP, high inter-model confidence occurs in 15 basins (63%), whereas in 8 basins (33%), moderate confidence inter-model confidence of projected changes is achieved. These differences can be partially attributed to structural variations among the models, including differences in process

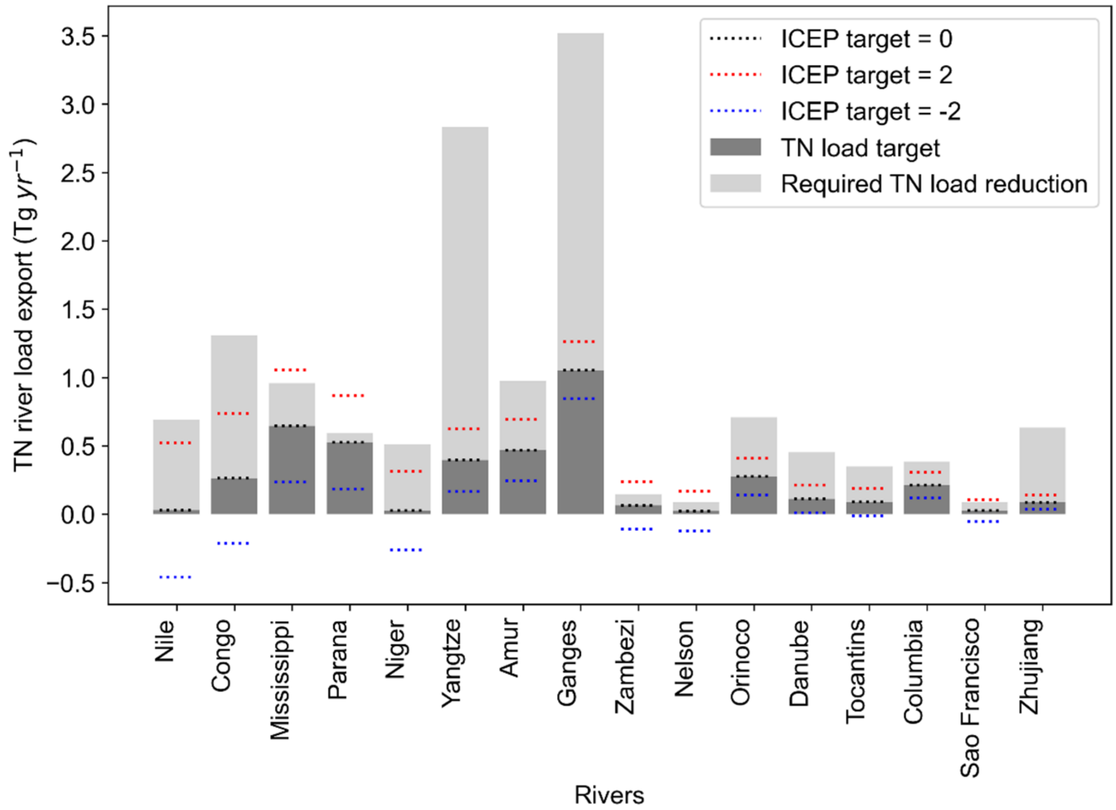

Figure 4. Targets for TN load export to oceans when ICEP = 0 (with uncertainty range from −2 to +2) under Global Orchestration (GO) scenario and SSP5-RCP8.5 for 2050, based on the mean of the three models. The Amazon, Ob, Yenisey, Lena, Mackenzie, St Lawrence, Mekong and Irrawaddy rivers are not shown because they do not need TN load reductions.

representation and the estimation of diffuse and point source inputs under scenario assumptions. Such variations also affect the predicted TN:TP ratios, reflecting how each model represents nutrient sources, cycling, and emerging contributions (e.g. aquaculture and nutrient legacies), and providing additional insight into the drivers of inter-model divergence. For instance; (i) MARINA-Multi operates at the sub-basin scale, IMAGE-DGNM at a 0.5° grid resolution, and CoSWAT-WQ at the HRU level. (ii) CoSWAT-WQ does not simulate dynamic land-use change beyond 2010, considering only changes in fertilizer and manure application while holding land use constant. This assumption may lead to inconsistencies in nutrient projections in regions experiencing substantial expansion of agricultural land or loss of natural land cover, which are captured by the other models. (iii) Both CoSWAT-WQ and MARINA-Multi do not account for nutrient legacies in groundwater, which are included in the IMAGE-DGNM model. (iv) IMAGE-DGNM model projects a growing dominance of aquaculture as an anthropogenic nutrient source by 2050, a factor not accounted for in the CoSWAT-WQ and MARINA-Multi models. Nevertheless, agricultural N and P inputs are expected to remain the primary drivers of nutrient export, as represented in these global models, driving the substantial projected increases by 2050, particularly across Europe, India, China, and Sub-Saharan Africa. In addition, sewage-derived N and P loads are projected to rise globally under SSP5, driven by the expansion of coastal megacities (Beusen *et al* 2022, Liu *et al* 2024).

Beyond the above highlighted differences, more distinctions in the main model assumptions and implementations of CoSWAT-WQ, IMAGE-DGNM and MARINA-Multi are given in table S1. Although these examples do not capture all model differences, such structural and process variations inevitably influence model outputs. Additionally, averaging model outputs can obscure spatial variability, especially when predicted changes, such as nutrient load changes, are heterogeneous. In such cases, the average output may underestimate the true extent of change, as localized variations may cancel each other. Another consideration is that, although each model has been independently validated at regional or basin scales, none has been uniformly calibrated at the global scale. As a result, discrepancies in parameterization can partly explain the differences in model estimates, underscoring the importance of coordinated model calibration and intercomparison frameworks for improving confidence in global nutrient assessments. Despite these uncertainties, using results from these multiple nutrient models

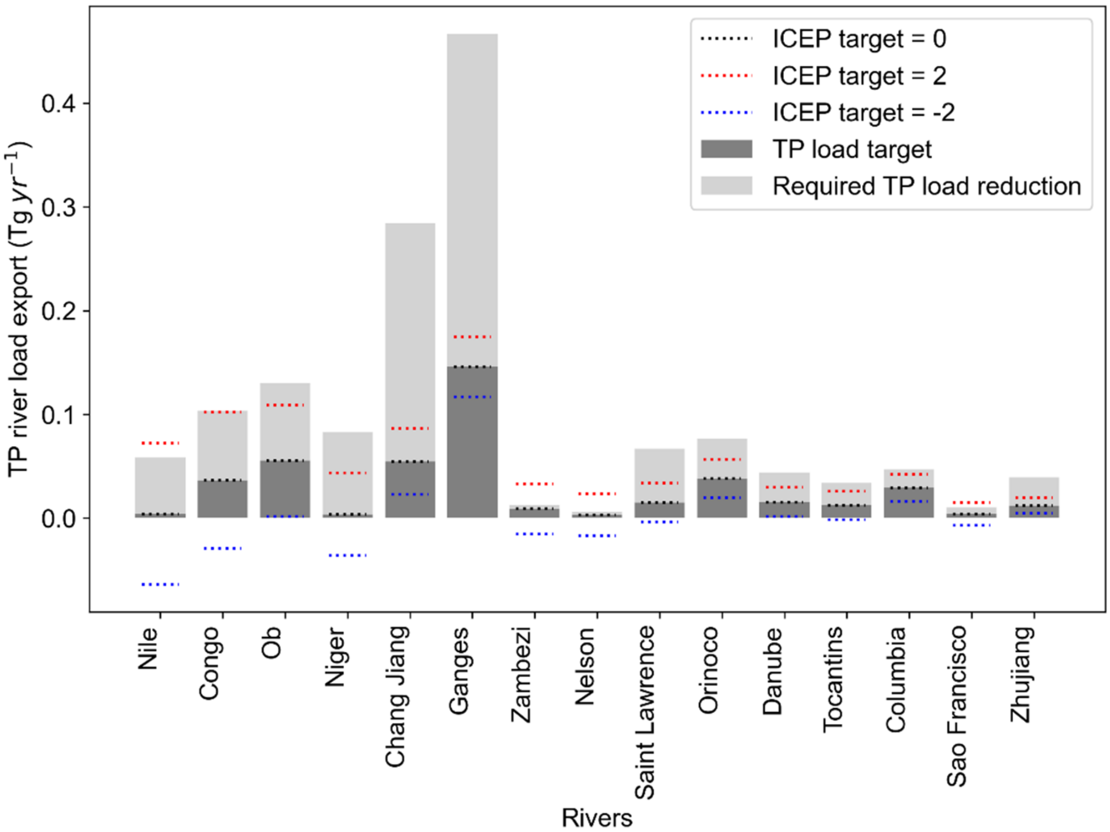

Figure 5. Targets for TP load export to oceans when ICEP = 0 (with uncertainty range from −2 to +2) under Global Orchestration (GO) scenario and SSP5-RCP8.5 for 2050, based on the mean of the three models. The Amazon, Mississippi, Parana, Yenisey, Lena, Amur, Mackenzie, Mekong and Irrawaddy are not shown because they do not need reductions.

provides a more broader perspective and comprehensive assessment of the robustness of identified pollution hotspots under certain future scenarios than results of a single water quality model. This also highlights the need for model intercomparison frameworks to assess uncertainties in projections (van Vliet *et al* 2019), such as the Inter-Sectoral Impact Model Intercomparison Project water quality community's protocol, which harmonizes model inputs and outputs for cross-scale climate change assessments (Strokal *et al* 2025).

4.3. Can the needed nutrient load reductions be achieved?

As few studies have quantified the nutrient load reductions required to protect coastal waters globally, there is limited opportunity to compare our results directly with the existing literature. Our study estimates that large reductions of riverine TN and TP loads are needed to prevent future coastal eutrophication under the SSP5-RCP8.5 scenario. Among the limited available studies, Ural-Janssen *et al* (2024) provide one of the few comparable assessments, focusing on the Danube River. While our estimates for the Danube suggest reductions of 75% for TN and 64% for TP riverine loads in 2050, Ural-Janssen *et al* (2024) project reductions of 69% for TDN and 26% for TDP for the same year. This discrepancy likely results from differences in the nutrient forms and input data considered. Our analysis includes both dissolved and particulate fractions (TN and TP), whereas Ural-Janssen *et al* (2024) focused solely on dissolved forms (TDN and TDP). Nevertheless, a consistent message emerges regarding the need for large nutrient load reductions in rivers to limit coastal eutrophication.

Potential strategies to reduce nutrient loads highlighted in literature include replacing synthetic nitrogen and phosphorus fertilizers with recycled manure, improving agricultural nutrient use efficiency, improving the quality of animal feed to reduce nitrogen content in manure, enhancing nutrient removal in wastewater treatment systems, and expanding wastewater infrastructure in regions such as Africa, where population growth is projected to significantly outpace other parts of the world. While some strategies are broadly applicable, their effectiveness could be specific to certain basins or geographical regions. However, determining the effectiveness of these interventions will require modeling of various scenarios and combinations of measures, as demonstrated by Li *et al* (2019) in their study on nutrient reduction pathways in China. Beyond technical feasibility, it is essential to assess the economic, social, and institutional feasibility of proposed measures to ensure their implementation is both practical and sustainable. For example, Baccour *et al* (2024) compare the economic viability of nutrient reduction strategies with that of water quantity management approaches in the Pearl river basin, showing that reducing nutrient loads could help alleviate pressure on water resources by 2050 under the SSP5-RCP8.5 scenario.

4.4. Limitations related to ICEP

A key data limitation of this study is the reliance on silica projections from Seitzinger *et al* (2010), the only available global dataset. These projections were developed under various future scenarios, and we used the GO scenario, which assumes a highly globalized world with rapid economic growth by 2050. However, this scenario may not fully align with the more recent SSP-based projections. While GO is the closest equivalent to SSP5, no other projected silica datasets are available for SSPs to our knowledge. Given that silica flux is central to the ICEP based analyses of eutrophication risk, further research is needed to improve silica observations and future simulations, that can potentially refine the estimates of the maximum allowable nutrient loads and enable ICEP applications in other river basins worldwide.

Another source of uncertainties related to ICEP is that it is based on the Redfield ratio of N:P:C:Si which is generic for the coastal ecosystem considering that other factors, such as water mixing, water depth, pH, light and water temperature may also be important (Li *et al* 2019). For example, ocean acidification will increase the elemental ratio of silicon and nitrogen by 17 $\pm$ 6% by 2100 due to lower chemical dissolution of silica, which will considerably alter the threshold Redfield ratio for diatom growth (Taucher *et al* 2022). As a result, nutrient limitation in coastal systems cannot be reliably inferred solely from the elemental ratios of nutrients delivered by rivers, since marine nutrient dynamics are influenced by a range of local conditions and processes (Billen and Garnier 2007).

Furthermore, the absence of a coupled land-ocean nutrient biogeochemical model limits our ability to assess how riverine nutrient inputs are transformed and transported in coastal and shelf seas. While our analysis provides estimates of TN, TP and silica exports from land to ocean, the ecological consequences of these fluxes depend critically on physical and biogeochemical processes in the receiving waters, including circulation, stratification, and internal nutrient cycling (Rabalais *et al* 2010, Fennel and Testa 2019). The same nutrient load can result in very different ecological outcomes depending on these factors, as well as climate-driven changes in ocean temperature (Cloern *et al* 2016, Breitburg *et al* 2018). Therefore, the nutrient reductions estimated in this study should be interpreted as first-order indicators for mitigating potential coastal eutrophication rather than as definitive thresholds. Future studies that couple terrestrial nutrient models with ocean biogeochemical models would allow for a more comprehensive assessment of downstream ecosystem responses and help inform targeted nutrient management strategies. However, while ICEP reflects characteristics of the river basin rather than the receiving marine waters, we consider it a useful foundation for exploring nutrient reduction strategies to marine waters.

5. Conclusions

This study highlights significant changes in nutrient loading across major global river basins by 2050, with substantial increases in TN and TP exports expected. Despite model uncertainties arising from structural differences and input data, the multi-model approach offers a solid foundation for identifying high-risk regions in need of nutrient load reduction. Backcasting analyses indicate that reducing total TN exports by 67% and TP exports by 64% for the selected rivers globally is essential to prevent coastal eutrophication. Rivers such as the Nile, Niger, Yangtze, Ganges, Danube, São Francisco, and Zhujiang will require considerable reductions exceeding 50% in both TN and TP to mitigate eutrophication risks effectively. These findings underscore the urgent need for nutrient reduction interventions to meet nutrient reduction targets and protect water quality. However, these measures must be evaluated in terms of their economic, social, and institutional feasibility to ensure practical and sustainable implementation. Given the uncertainties and limitations of our study, future research should focus on refining model consistency and data quality, particularly regarding silica, and explore multiple intervention scenarios to inform effective strategies for addressing nutrient pollution amidst global change.

Acknowledgment

This research was supported by the SOS-Water project (Grant Agreement No. 101059264), the EUROLakes project (Grant Agreement No. 01157482) and the ACT4CAP27 project (Grant Agreement

No. 101134874), all funded by the European Union's Horizon Europe research and innovation programme. K.S and I.M. were funded by the European Union's Horizon 2021 research and innovation programme under the Marie Sklodowska-Curie Grant Agreement No. 956623, MSCA-ITN-ETN-European Training Network (inventWater Project). M.T.N and A.v.G were supported by the AXA Research Chair fund on Water Quality and Global change.

Data availability statement

All global water quality simulations used in this study are available under the ISIMIP Water quality sector protocol (www.isimip.org/). Silica data was obtained from Seitzinger *et al* (2010).

Supplementary data available at https://doi.org/10.1088/3033-4942/ae54c3/data1.

Author contributions

Albert Nkwasa 0000-0002-8685-8854
Conceptualization (lead), Data curation (lead), Formal analysis (lead), Investigation (lead), Methodology (lead), Validation (lead), Visualization (lead), Writing – original draft (lead), Writing – review & editing (lead)

Maria Theresa Nakkazi 0000-0002-3171-1687
Data curation (supporting), Formal analysis (supporting), Writing – review & editing (supporting)

Celray James Chawanda
Data curation (supporting), Writing – original draft (supporting), Writing – review & editing (supporting)

Ting Tang 0000-0002-2867-9241
Visualization (supporting), Writing – original draft (supporting), Writing – review & editing (supporting)

Keerthana Suresh 0000-0003-1930-9318
Conceptualization (supporting), Writing – original draft (supporting), Writing – review & editing (supporting)

Arthur H W Beusen
Conceptualization (supporting), Data curation (supporting), Formal analysis (supporting), Writing – original draft (supporting), Writing – review & editing (supporting)

Ilaria Micella 0000-0003-0442-5121
Data curation (supporting), Formal analysis (supporting), Resources (supporting), Writing – original draft (supporting), Writing – review & editing (supporting)

Taher Kahil 0000-0002-7812-5271
Funding acquisition (lead), Project administration (supporting), Resources (supporting), Writing – original draft (supporting), Writing – review & editing (supporting)

Ann van Griensven
Conceptualization (supporting), Formal analysis (supporting), Writing – original draft (supporting), Writing – review & editing (supporting)

References

Arnold J G, Srinivasan R, Muttiah R S and Williams J R 1998 Large area hydrologic modeling and assessment part I: model development[1] *J. Am. Water Resour. Assoc.* **34** 73–89

Baccour S, Goelema G, Kahil T, Albiac J, van Vliet M T H, Zhu X and Strokal M 2024 Water quality management could halve future water scarcity cost-effectively in the Pearl River Basin *Nat. Commun.* **15** 5669

Bak M P, Micella I, Jones E R, Kumar R, Nkwasa A, Tang T, van Vliet M T H, Wang M and Strokal M 2025 Future river exports of nutrients, plastics, and chemicals worldwide under climate-driven hydrological changes *Environ. Res. Lett.* **20** 094033

Best J 2019 Anthropogenic stresses on the world's big rivers *Nat. Geosci.* **12** 7–21

Beusen A H W, Doelman J C, Van Beek L P H, Van Puijenbroek P J T M, Mogollón J M, Van Grinsven H J M, Stehfest E, Van Vuuren D P and Bouwman A F 2022 Exploring river nitrogen and phosphorus loading and export to global coastal waters in the Shared Socio-economic pathways *Glob. Environ. Change* **72** 102426

Beusen A H W, Van Beek L P H, Bouwman A F, Mogollón J M and Middelburg J J 2015 Coupling global models for hydrology and nutrient loading to simulate nitrogen and phosphorus retention in surface water–description of IMAGE–GNM and analysis of performance *Geosci. Model. Dev.* **8** 4045–67

Bieger K, Arnold J G, Rathjens H, White M J, Bosch D D, Allen P M, Volk M and Srinivasan R 2017 Introduction to SWAT+, a completely restructured version of the soil and water assessment tool *J. Am. Water Resour. Assoc.* **53** 115–30

Billen G and Garnier J 1997 The Phison River plume: coastal eutrophication in response to changes in land use and water management in the watershed *Aquat. Microb. Ecol.* **13** 3–17

Billen G and Garnier J 2007 River basin nutrient delivery to the coastal sea: assessing its potential to sustain new production of non-siliceous algae *Mar. Chem.* **106** 148–60

Billen G and Garnier J 2023 The water-agro-food system: upscaling from the Seine river basin to the global scale *C. R. Géosci.* **355** 301–15

Breitburg D *et al* 2018 Declining oxygen in the global ocean and coastal waters *Science* **359** eaam7240

Brown L C and Barnwell T O 1987 The enhanced stream water quality models QUAL2E and QUAL2E-UNCAS: documentation and user model *Environmental Research Laboratory* (Office of Research and Development, U.S. Environmental Protection Agency)

Cloern J E *et al* 2016 Human activities and climate variability drive fast-paced change across the world's estuarine–coastal ecosystems *Glob. Change Biol.* **22** 513–29

de Klein J J M and Koelmans A A 2011 Quantifying seasonal export and retention of nutrients in West European lowland rivers at catchment scale *Hydrol. Process.* **25** 2102–11

Diaz R, Selman M and Chique C 2011 *Global Eutrophic and Hypoxic Coastal Systems* (World Resources Institute)

Elsayed H, Beusen A and Bouwman A F 2025 Nutrient transport from the Ganga–Brahmaputra–Meghna River system to the Bay of Bengal: past and future trends *Environ. Res. Lett.* **20** 024054

Fennel K and Testa J M 2019 Biogeochemical controls on coastal hypoxia *Annu. Rev. Mar. Sci.* **11** 105–30

Fink G, Alcamo J, Flörke M and Reder K 2018 Phosphorus loadings to the world's largest lakes: sources and trends *Glob. Biogeochem. Cycles* **32** 617–34

Garnier J, Beusen A, Thieu V, Billen G and Bouwman L 2010 N:P:Si nutrient export ratios and ecological consequences in coastal seas evaluated by the ICEP approach *Glob. Biogeochem. Cycles* **24** 2009GB003583

Gomi K, Ochi Y and Matsuoka Y 2011 A systematic quantitative backcasting on low-carbon society policy in case of Kyoto city *Technol. Forecast. Soc. Change* **78** 852–71

Green P A, Vörösmarty C J, Meybeck M, Galloway J N, Peterson B J and Boyer E W 2004 Pre-industrial and contemporary fluxes of nitrogen through rivers: a global assessment based on typology *Biogeochemistry* **68** 71–105

Grizzetti B, Bouraoui F and De Marsily G 2008 Assessing nitrogen pressures on European surface water *Glob. Biogeochem. Cycles* **22** GB4023

Kemp W M, Testa J M, Conley D J, Gilbert D and Hagy J D 2009 Temporal responses of coastal hypoxia to nutrient loading and physical controls *Biogeosciences* **6** 2985–3008

Knutti R, Furrer R, Tebaldi C, Cermak J and Meehl G A 2010 Challenges in combining projections from multiple climate models *J. Clim.* **23** 2739–58

Li A, Strokal M, Bai Z, Kroeze C and Ma L 2019 How to avoid coastal eutrophication—a back-casting study for the North China Plain *Sci. Total Environ.* **692** 676–90

Liu X, Beusen A H W, van Puijenbroek P J T M, Zhang X, Wang J, van Hoek W J and Bouwman A F 2024 Exploring wastewater nitrogen and phosphorus flows in urban and rural areas in China for the period 1970–2015 *Sci. Total Environ.* **907** 168091

Maher N, Power S B and Marotzke J 2021 More accurate quantification of model-to-model agreement in externally forced climatic responses over the coming century *Nat. Commun.* **12** 788

Malagó A, Bouraoui F, Vigiak O, Grizzetti B and Pastori M 2017 Modelling water and nutrient fluxes in the Danube River Basin with SWAT *Sci. Total Environ.* **603–604** 196–218

Maúre E D R, Terauchi G, Ishizaka J, Clinton N and DeWitt M 2021 Globally consistent assessment of coastal eutrophication *Nat. Commun.* **12** 6142

Mayorga E, Seitzinger S P, Harrison J A, Dumont E, Beusen A H W, Bouwman A F, Fekete B M, Kroeze C and Van Drecht G 2010 Global nutrient export from WaterSheds 2 (NEWS 2): model development and implementation *Environ. Model. Softw.* **25** 837–53

McDowell R W, Luo D, Pletnyakov P, Upsdell M and Dodds W K 2025 Anthropogenic nutrient inputs cause excessive algal growth for nearly half the world's population *Nat. Commun.* **16** 1830

Micella I, Kroeze C, Bak M P and Strokal M 2024a Causes of coastal waters pollution with nutrients, chemicals and plastics worldwide *Mar. Pollut. Bull.* **198** 115902

Micella I, Kroeze C, Bak M P, Tang T, Wada Y and Strokal M 2024b Future scenarios for river exports of multiple pollutants by sources and sub-basins worldwide: rising pollution for the Indian Ocean *Earths Fut.* **12** e2024EF004712

Milliman J D and Farnsworth K L 2011 *River Discharge to the Coastal Ocean: A Global Synthesis* (Cambridge University Press, Cambridge) (https://doi.org/10.1017/CBO9780511781247)

Nkwasa A, Chawanda C J, Jägermeyr J and van Griensven A 2022 Improved representation of agricultural land use and crop management for large-scale hydrological impact simulation in Africa using SWAT+ *Hydrol. Earth Syst. Sci.* **26** 71–89

Nkwasa A, James Chawanda C, Theresa Nakkazi M, Tang T, Eisenreich S J, Warner S and van Griensven A 2024 One third of African rivers fail to meet the'good ambient water quality' nutrient targets *Ecol. Indic.* **166** 112544

Nkwasa A, James Chawanda C, Theresa Nakkazi M and van Griensven A 2025 CoSWAT-WQ v1.0: a high-resolution community global SWAT+ water quality model *EGUsphere* 1–19

O'Neill B C *et al* 2017 The roads ahead: narratives for shared socioeconomic pathways describing world futures in the 21st century *Glob. Environ. Change* **42** 169–80

Rabalais N N, Díaz R J, Levin L A, Turner R E, Gilbert D and Zhang J 2010 Dynamics and distribution of natural and human-caused hypoxia *Biogeosciences* **7** 585–619

Redfield A C, Ketchum B H and Richards F A 1963 The influence of organisms on the composition of sea-water *The Sea* (*The Composition of Sea-Water Comparative and Descriptive Oceanography*) vol 2, ed M N Hill (Interscience Publishers) pp 26–77

Robinson J B 1990 Futures under glass: a recipe for people who hate to predict *Futures* **22** 820–42

Rousseau V, Becquevort S, Parent J-Y, Gasparini S, Daro M-H, Tackx M and Lancelot C 2000 Trophic efficiency of the planktonic food web in a coastal ecosystem dominated by *Phaeocystis* colonies *J. Sea Res.* **43** 357–72

Seitzinger S P *et al* 2010 Global river nutrient export: a scenario analysis of past and future trends *Glob. Biogeochem. Cycles* **24** GB0A08

Seitzinger S P, Harrison J A, Dumont E, Beusen A H W and Bouwman A F 2005 Sources and delivery of carbon, nitrogen, and phosphorus to the coastal zone: an overview of Global Nutrient Export from Watersheds (NEWS) models and their application *Glob. Biogeochem. Cycles* **19** GB4S01

Sharples J, Middelburg J J, Fennel K and Jickells T D 2017 What proportion of riverine nutrients reaches the open ocean? *Glob. Biogeochem. Cycles* **31** 39–58

Strokal M *et al* 2025 Advancing water quality model intercomparisons under global change: perspectives from the new ISIMIP water quality sector *Environ. Res. Water* **1** 035002

Strokal M, Kroeze C, Wang M, Bai Z and Ma L 2016 The MARINA model (model to assess River inputs of nutrients to seAs): model description and results for China *Sci. Total Environ.* **562** 869–88

Sutanudjaja E H *et al* 2018 PCR-GLOBWB 2: a 5 arcmin global hydrological and water resources model *Geosci. Model. Dev.* **11** 2429–53

Taucher J, Bach L T, Prowe A E F, Boxhammer T, Kvale K and Riebesell U 2022 Enhanced silica export in a future ocean triggers global diatom decline *Nature* **605** 696–700

Tong Y, Zhao Y, Zhen G, Chi J, Liu X, Lu Y, Wang X, Yao R, Chen J and Zhang W 2015 Nutrient loads flowing into coastal waters from the main rivers of China (2006–2012) *Sci. Rep.* **5** 16678

UNEP 2021 Understanding the state of the ocean: a global manual on measuring SDG 14.1.1, SDG 14.2.1 and SDG 14.5.1 URL (available at: https://wedocs.unep.org/handle/20.500.11822/35086) (Accessed 24 February 2025)

Ural-Janssen A, Kroeze C, Meers E and Strokal M 2024 Large reductions in nutrient losses needed to avoid future coastal eutrophication across Europe *Mar. Environ. Res.* **197** 106446

van Vliet M T H, Franssen W H P, Yearsley J R, Ludwig F, Haddeland I, Lettenmaier D P and Kabat P 2013 Global river discharge and water temperature under climate change *Glob. Environ. Change* **23** 450–64

van Vliet M T *et al* 2019 Model inter-comparison design for large-scale water quality models *Curr. Opin. Environ. Sustain.* **36** 59–67

Van Vuuren D P *et al* 2011 The representative concentration pathways: an overview *Clim. Change* **109** 5

Yasin J A, Kroeze C and Mayorga E 2010 Nutrients export by rivers to the coastal waters of Africa: past and future trends *Glob. Biogeochem. Cycles* **24** GB0A07